Vol. 91 No. 6 pp. 2230–2242 ACTA GEOLOGICA SINICA (English Edition) Dec. 2017

Burial History and Petroleum Entrapment in the Yaoyingtai Region of the Changling Fault Depression, China

YANG Guang[1,*], LIU Changli[1], FAN Jiarui[2] and CHEN Peng[3]

1 *College of Earth Sciences, Jilin University, Changchun 130061, Jilin, China*
2 *Dalian Branch, China Railway No.9 group Co. Ltd., Dalian 116000, Liaoning, China*
3 *D&P Technology Research Institute, PetroChina Liaohe Oilfield Company, Panjin 124010, Liaoning, China*

Abstract: This work aims to reconstruct the burial history of various kinds of sandstones penetrated by the well YS201 in the Yaoyingtai region of the Changling Fault Depression, southern Songliao Basin, China. Analyses of fluid inclusions in the reservoir rocks, combined with a review of the regional tectonic evolution, revealed the hydrocarbon accumulation stage and accumulation age of the Early Cretaceous Denglouku group and the first member of the Quantou group reservoir, which are the future exploration focus for deep gas reservoirs in this region. Acoustic time data and sedimentary rates calculated for sediments in the YS201 well yielded thicknesses for the Yingcheng, Nenjiang, and Mingshui groups of 506, 539.18, and 144.85 m, respectively, thereby revealing the burial history of the sediments in the well. Fluid inclusions of the Denglouku group reservoir and the first member of the Quantou group reservoir contain oil inclusions and hydro-carbonaceous salt water inclusions. The main peaks of the homogenization temperature and salinity of these saltwater inclusions in the first member of the Quantou group reservoir are generally 110–120°C and 6wt%–8wt%, respectively, and for the Denglouku group are 130–140°C and 4wt%–6wt%. The data for both reservoirs show only one main peak, indicating that they both have experienced single-stage accumulation. Combining the homogenization temperature of the reservoir fluid inclusions with the burial and thermal history of the sediments in the YS201 well, we infer that the hydrocarbon gas in these two intervals accumulated at 79 Ma (middle Late Cretaceous).

Key words: Songliao Basin, Yaoyingtai region, reservoir fluid inclusion, denudation thickness, accumulation stage, accumulation age

1 Introduction

An understanding of the geological history of a reservoir is a basic requirement for petroleum exploration (Punanova et al., 2006; Lee et al., 2004; Dodds, 2000; Ingram et al., 2004). Reservoir development is an important factor in the selection of an exploration area and for the potential success of a target layer. Burial history is a fundamental part of studying hydrocarbon accumulation, and restoring the denuded thicknesses in a study area is the key to burial history research (Kemp et al., 2005; Tokatli et al., 2006; Blamey et al., 2014; Grobe et al., 2015; English et al., 2016). The methods used to restore the formations in a sedimentary basin and to calculate the denudation thickness at an unconformity can be roughly divided into four types: geothermic method based on the ancient scale method, geological method based on the principles of stratigraphy and sedimentology, geophysical method based on well logging and seismic data, and geochemical method based on the principle of chemical distribution or accumulation (Lastett et al., 1987; Carter et al., 2000; Henry, 1996). Each method has their own limitations according to regional basin development and tectonic history of the area. The most effective method to estimate denudation thickness can be selected based on the characteristics of the basin of interest.

A series of analyses was undertaken to select the most appropriate research method for investigating the well YS201. (1) To satisfy the basic condition that the upper structural layer experiences higher paleogeothermal

* Corresponding author. E-mail: yg@jlu.edu.cn

conditions than the lower layer, we conducted paleogeothermal vitrinite reflectance and apatite fission track analyses to determine the paleogeothermal gradient, but the analyzed layers are too deep for this method (Xiang Caifu et al., 2007). (2) Meso-Cenozoic sedimentary basin compaction laws were generally apparent, meaning that porosity analysis and acoustic time data yield reliable results. Therefore, we can use the porosity of a sedimentary basin, combining with acoustic time data, to estimate the denudation thickness of sedimentary strata. (3) For poly–cyclic superposed basins of the Phanerozoic, the sedimentary and tectonic evolution of the basins should first be analyzed in detail. Then, the stratigraphic contrast method should be used to determine the range of denudation. Finally, a combination of geothermic analysis and data on depositional fluctuations was used to calculate the definite value of the denuded thickness (Yuan Yusong et al., 2008).

The Yaoyingtai region of the Songliao Basin is characteristic of Meso–Cenozoic sedimentary basins in that strata compaction laws are generally apparent and the relationship between acoustic time and depth appears to have remained unchanged during the denudation of strata. Through the acoustic time method and sedimentary rate method, combined with sedimentation rates, the denuded thickness of the Yingcheng, Nenjiang, and Mingshui groups can be estimated.

The geological processes which lead to reservoir development are important in understanding hydrocarbon accumulation within a basin (Karlsen et al., 1993; Nedkvitne et al., 1993). Accurate analysis of multiphase tectonic events is required, as geological structures can influence migration and control the location of accumulations within the basin (Du Letian et al., 2015; Pang Xiongqi et al., 2015). Understanding the tectonic history therefore improves the efficiency of hydrocarbon exploration, as the distribution of hydrocarbon reservoir can be more accurately predicted. The main phases of reservoir development are source rock deposition, reservoir maturation, and trap formation (He Bizhu et al., 2016). Study of these phases of reservoir development reveals numerous variables, including tectonic events (Ma Yongsheng et al., 2016; Wang Pujun et al., 2007), burial history (Sachse et al., 2016; Premarathne et al., 2016), thermal evolution (Raznitsin, 2014; Karimpouli et al., 2013), and digenetic history. Analyses of the geological history may provide direct geochemical evidence of hydrocarbon accumulation, such as studies of reservoir fluid inclusions (Liu Dehan, 1995; Zheng Youye et al., 1998；Zou Caineng et al., 2007), the dating of digenetic minerals, and analyses of reservoir bitumen (Mark et al., 2006; Mark et al., 2005).

This study examines reservoir fluid inclusions in order to determine the age of hydrocarbon accumulation. The reservoir fluids in inclusions enable the age of hydrocarbon accumulation to be established, and they also indicate the chemistry, temperature, and pressure conditions during accumulation. These reservoir fluid inclusions are generally unaffected by later secondary changes in the oil reservoir and offer an effective way to understand the relevant geological processes (Burruss et al., 1983; Haszeldine et al., 1984). The study mainly used homogenization temperatures, salinity, and laser Raman spectra of reservoir fluid inclusions, combining with data of burial history, deposition rates, and the calculated hydrocarbon accumulation stage for the first member of the Quantou group and the Denglouku group to aid our understanding of the reservoir history. The results indicate potential layers for gas reservoir exploration (Lethaeuser et al., 1989; Zhao Mengjun et al., 2004; Jones et al., 2000; Kelly, et al., 2000).

2 Geological Setting and Petroleum Geological Characteristics

The Meso-Cenozoic Songliao Basin, located in northeast China, is one of China's largest inland fault-depression lacustrine basins (Ge Rongfeng et al., 2010). The basin is 750 km long and 330–370 km wide, with a total surface area of >260,000 km^2. The Changling fault depression is located in the south of the Songliao Basin, and the Yaoyingtai region, studied here, is located in the southern Chaganhua sub-sag and Daerhan fault complex (Fig. 1). The fault structure is N–S trending, has a westward–facing monoclinal form, and is 420 km^2 in area (Chen Juan et al., 2008; Li Zongquan et al., 2008). The formations in the basin are (from oldest to youngest) the Jurassic Huoshiling group (J_3h); the Lower Cretaceous Shahe group (K_1sh), Yingcheng group (K_1yc), Denglouku group (K_1d), and Quantou group (K_1q, this group is divided into four members); the Upper Cretaceous Qingshankou group (K_2qn), Yaojia group (K_2y), Nenjiang group (K_2n), Sifangtai group (K_2s), and Mingshui group (K_2m); and the Neogene Taikang group (N*t*). This study concentrates on the Denglouku group and the first member of Quantou group.

The Songliao Basin has experienced three episodes of tectonic movement: the end of the Yingcheng tectonic event, equivalent to phase III of the Yanshanian movement, which led to uplift and faulting across the study area; the end of the Late Cretaceous Nenjiang tectonic event, which affected the whole basin and caused uplift across the study area; and the Late Cretaceous uplift during deposition of the youngest sediments of the

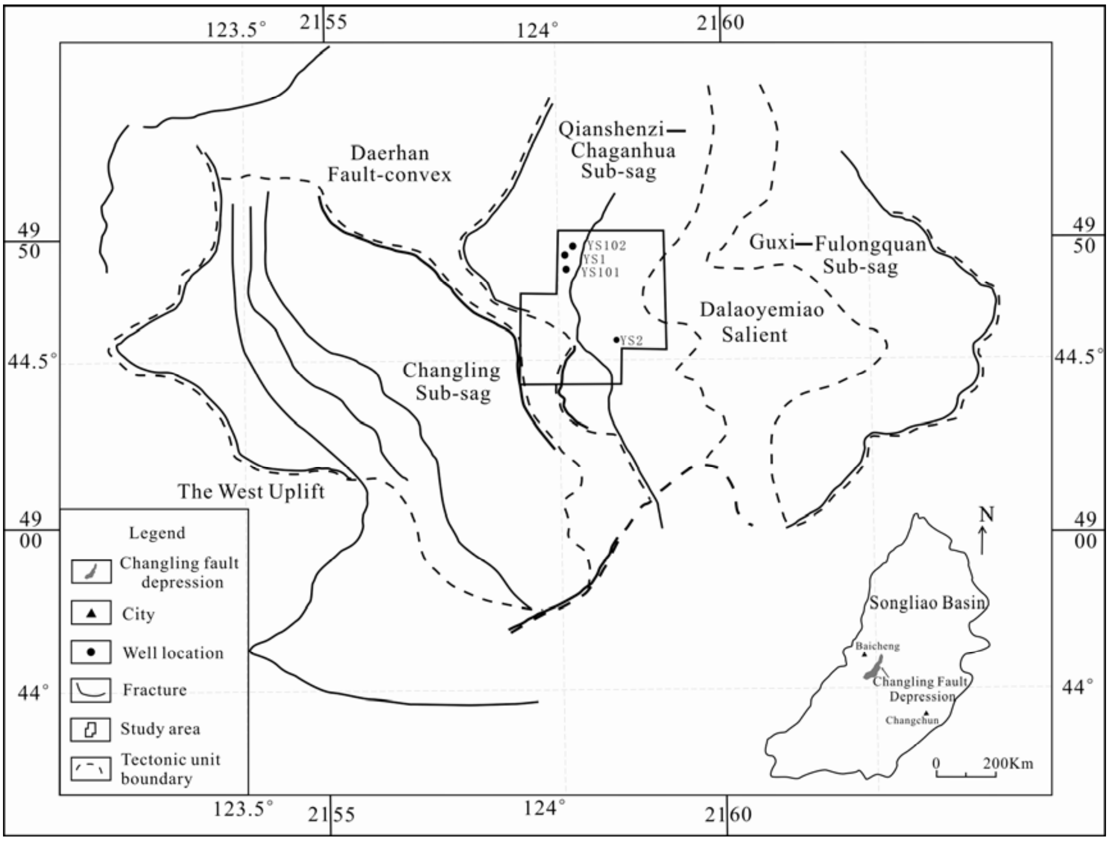

Fig. 1. Map showing division of deep tectonic units in the south of the Changling fault depression.

Mingshui group, which led to localized intense faulting, uplift, and denudation. The final period of uplift had less impact on the study area than the previous two events. Intense tectonic movements have a significant controlling effect on the hydrocarbon accumulation (Zhao Wenzhi et al., 2004). The Yaoyingtai region is located between two sub-sags, and this uplifted area is a favorable structure for hydrocarbon migration and accumulation (Wang Yougong et al., 2014; Hu Ming et al., 2010).

3 Analytical Methods and Analytical Results

3.1 Calculation of denudation thickness and reconstruction of burial history from a single drill hole

Existing drill holes and seismic data indicate that the study area was affected by the late Nenjiang and late Yingcheng tectonic events, both of which involved uplift that led to erosion. Seven drill holes exist within the study area, and the combined drill hole information could be used to calculate the denudation thickness from acoustic time data. The homogenization temperatures of reservoir fluid inclusions were determined from wells located near the YS201 well; consequently, the burial history of the YS201 well can be used to represent the overall burial history for the Yaoyingtai region.

3.1.1 Denudation thickness of the Nenjiang group calculated using the acoustic time method

The Songliao Basin is a Meso–Cenozoic basin in which the formation compaction law is well observed, and the acoustic time method can thus be used to calculate the denudation thickness. By utilizing lithology data from the drill holes logs, we can extract acoustic time data for the mudstone of the Nenjiang group and construct a time–depth curve, thereby yielding a compaction curve (equation (1)). The same method is used to construct another time–depth curve for the strata (Sifangtai group) that lie across the surface of denuded strata (Liu Jingyan et al., 2000). The compaction curve is calculated as follows:

$$T = (T_0 - c)\exp(-bx) + c \tag{1}$$

Where T and x represent the acoustic propagation time of logging data and formation depth, respectively; T_0 is the travel time of the acoustic wave near the surface (in water); and b and c are unknowns that are calculated using best fit values via statistical methods. b represents the compact law in the compaction curve, and c represents the propagation time of acoustic waves in rock; its value depended on the lithology, porosity, and pore fluid. Laboratory studies have shown that the propagation time of acoustic waves in rock is generally 128–233 μs/m. Therefore, based on the characteristics of the rock strata and for reasonable physical conditions, c can be estimated and subsequently b can be calculated. Once appropriate values for b and c have been determined, a reasonable compaction curve equation can then be established. By using the comparison of the slopes and positions of the two time–depth curves for the Nenjiang group and for the Sifangtai group, we infer that the acoustic time method is accurate in terms of calculating denudation thickness (Mu Zhonghai et al., 2000; Chen Ruiyin et al., 2006). As shown in Fig. 2, the slope of the compaction curve for the older strata (the Nenjiang group) is greater than that for the younger strata (the Sifangtai group), indicating that the compaction of sediments across the unconformity surface was continuous; therefore, we can use the acoustic time method to restore the denuded thickness. A correlation coefficient is generally used to evaluate the strength of a relationship between two variables. The equation (1) is calculated as follows:

$$\ln (T-c) = (T_0-c) - bX$$

The equation is converted into a linear equation $Y=mX+n$, with T_0 taken from the range 620–650 μs/m. The

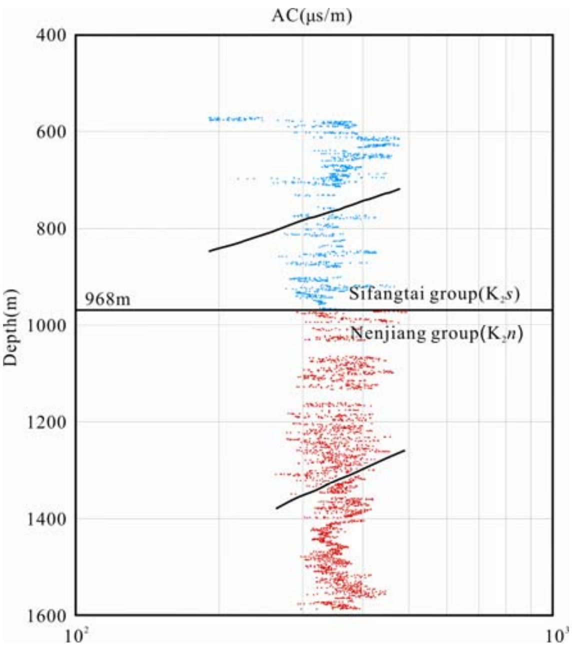

Fig. 2. Acoustic time–depth fitting graphs of the YS201 well.

original thickness of the Nenjiang group is calculated to be 1161.63 m, compared with a present thickness of 622.45 m. The difference between these two values is the amount of denudation; therefore, a 539.18 m thickness of sediment has been eroded from the Nenjiang group.

3.1.2 Sedimentation rate method used to calculate the denuded thickness of the Yingcheng and Mingshui groups

Lithological data taken from the drill hole logs indicate that the Yingcheng group comprises a series of volcanic rocks, mostly grey and brown rhyolite and light brown volcanic breccia. The group does not contain mudstone, meaning we are unable to use the acoustic time method to estimate the denudation thickness. An alternative approach is to use the sedimentation rates combined with duration of denudation to calculate the thickness of denuded strata during this period (Tan Kaijun et al., 2004; Ken et al., 2008). The denudation duration is the difference in age between the strata immediately above and below the erosional boundary; i.e., $T_e - T_i$. Previous studies have estimated deposition rates for the Yingcheng and Mingshui groups of 270 and 211 m/Ma, respectively (Guo Wei et al., 2009). The age of the Yingcheng group spans from 136 to 124 Ma, and the age of the Mingshui group spans from 67.7 to 65 Ma (Table 1). The denudation thickness of the Yingcheng and Mingshui groups is determined as 506 m and 144.85 m, respectively, as obtained using the following equation (2):

$$(H_i+2H_e)/(T_{i+1}-T_i) = H_e/(T_e-T_i) \quad (2)$$

Where T_e is the onset age of erosion, Ma; H_e is the thickness of eroded strata, m; T_{i+1} is geological age of the lower boundary of eroded strata, Ma; H_i is residual thickness of eroded strata, m; T_i is geological age of upper boundary of eroded strata, Ma.

3.2 Calculating the age of onset of denudation

If the thickness of eroded strata, the residual thickness, and the geological age of the upper and lower unconformity surfaces are known, we can calculate the beginning time of the erosion period. The onset age of

Table 1 Statistics of the denudation thickness of the YS201 well

Geological age	Depth of lower boundary (m)	Strata thickness (m)	Geological age of lower boundary (Ma)	Denudation thickness (m)	Beginning age of denudation (Ma)
Nt	290	150	6	0	—
K_2m	570	280	67.7	144.85	65.7*
K_2s	968	398	73	0	—
K_2n	1590.45	622.45	84	539.18	76.5*
K_2y	1692	101.55	88.5	0	—
K_2qn	2315.4	623.4	100	0	—
K_1q	3379	1063.6	112	0	—
K_1d	3892	513	124	0	—
K_1yc	4500	608	136	506	125.9*

Note: *The values are obtained by rounding retained to one decimal place.

erosion was determined according to equation (2), by combining denudation thickness data, the geological age of the upper boundary of eroded strata, and the residual thickness of the Nenjiang, Yingcheng, and Mingshui groups (Table 1). The calculated age of denudation onset for the Yingcheng group is 125.9 Ma, for the Nenjiang group is 76.5 Ma, and for the Mingshui group is 65.7 Ma.

3.3 Reconstruction of the burial history

The term 'burial history' refers to the complete stratigraphy of a basin sedimentary unit or a series of units (sequence and group) from the original depositional environment to the present time or a certain geological period. This study used the inversion backstripping method to reconstruct the burial history. The main principle of backstripping method is to reconstruct the stratigraphy from the residual layer, working through the geological history, stripping step by step, until the pre-erosional situation is achieved, while the compacted thickness of each layer remains unchanged. With the increasing burial depth, the overburden loading on older formations increases, meaning that porosity decreases and volume decreases. We can assume that the lateral position of the formation remains unchanged during the sedimentation process and only the longitudinal position changes. During the process of compaction, the formation volume decreases, and the formation thickness also decreases. According to the assumption that the sedimentation rate remains constant, the compacted thickness does not change across the area except in response to geological events such as faulting and denudation. The calculation for the stripping method includes three factors: the compacted thickness of the formation, the original un–compacted formation thickness, and the thickness of the formation in each geological period. The backstripping process, therefore, is required to solve three problems, as follows. (1) The first problem arises from the principle of sedimentary compaction, by using the porosity–depth curve across the study area and burial depths to calculate the thickness of the compacted thickness. (2) The thickness of the original un–compacted formation when the burial depth is 0 m can be derived from the compacted thickness and the porosity–depth curve. (3) For each formation (except for the structural layer), under the condition that its skeleton thickness (compacted thickness) remains unchanged, since nowadays the embedded depth of stratum status, step by step stripping is applied until the pre-erosional situation is achieved; the burial depth of each formation can then be calculated (Yan Baozhen et al., 2006). Employing the compaction coefficients of the sandstone and mudstone porosity–depth curves in the YS201 well, and utilizing the 'peeling back mathematical model' proposed by Yan Baozhen et al. (2006), the ancient burial depth of the stratum is calculated (Table 2). Combining the calculated ancient buried depth, and the denudation thickness and

Table 2 Recovery burial history data of YS201 well

Formation	Geological age	Sandstone content	Mudstone content	Formula of sandstone porosity-depth curve	Formula of mudstone porosity-depth curve	Skeleton thickness (m)	Paleo-buried depth (m)
Mingshui group	K_2m	—	—	—	—	570	570
Sifangtai group	K_2s	0.4824	0.495	$y=0.762e^{-0.0009x}$	$y=0.020e^{0.0082x}$	324.68	465
Nenjiang group	K_2n	0.204	0.7679	$y=0.7883e^{-0.0007x}$	$y=0.439e^{-0.0001x}$	369.41	677
Yaojia group	K_2y	0.128	0.7976	$y=0.801e^{-0.0007x}$	$y=2.934e^{-0.0015x}$	97.83	126
Qingshankou group	K_2qn	0.2727	0.7154	$y=2.729e^{-0.0015x}$	$y=15.56e^{-0.0024x}$	594.29	633.5
Quantou group	K_1q	0.4757	0.5156	$y=0.4022e^{-0.0007x}$	$y=0.3594e^{-0.0005x}$	860.22	1179
Denglouku group	K_1d	0.4739	0.501	$y=0.2954e^{-0.0005x}$	$y=0.3978e^{-0.0005x}$	427.85	605
Yingcheng group	K_1yc	0	0	—	—	382.81	617.8

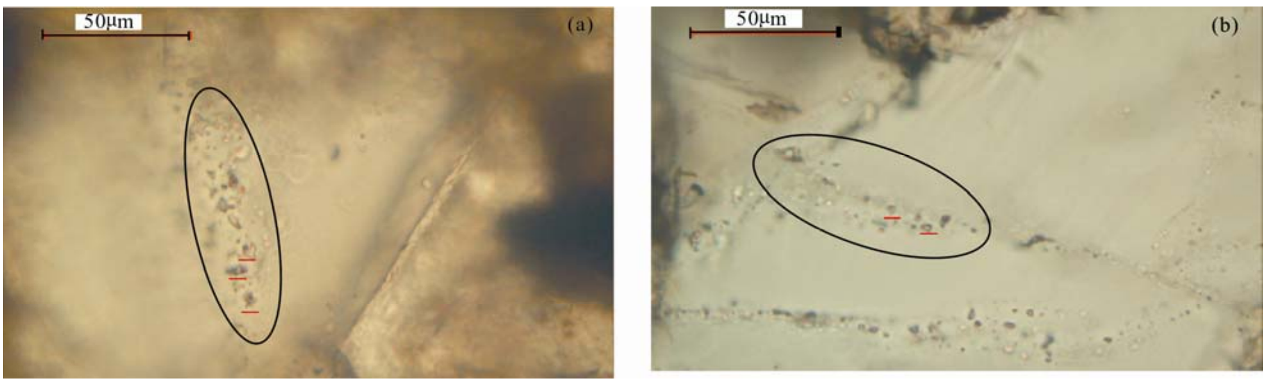

Fig. 3. Distribution of fluid inclusions under microscope.
(a), Fluid inclusions from 3278.35 m in the first member of Quantou Formation of YS102 well; (b), Fluid inclusions from 3714.74m in Denglouku Formation of YS2 well.

onset time (Table 1) for each of the Yingcheng, Nenjiang, and Mingshui groups, we can reconstruct the burial history for the sediments in the YS201 well (Fig. 6).

4 Analysis of Reservoir Fluid Inclusions

The fluid (oil, gas, water) in fluid inclusions was captured and sealed within the crystal lattice of authigenic mineral or within healing digenetic micro–fractures. These inclusions record the original chemistry of fluids at different stages of diagenesis. The inclusions record the composition and properties of water and hydrocarbon, and the physical and chemical conditions during the different phases of hydrocarbon filling of the reservoir (Bhattacharya et al., 2014). The preservation of these inclusions allows us to gain homogenization temperatures to study the hydrocarbon filling period and the accumulation time of the reservoir (Bhullar et al., 1999; Goldstein, 2001; Chi Guoxiang et al., 2003; Munz et al., 2004). This work used laser Raman spectroscopy to determine whether inclusions contain hydrocarbon signatures. We then measured fluid inclusion homogenization temperatures and salinity to determine the hydrocarbon accumulation stage and age in the Yaoyingtai region.

4.1 Fluid inclusion characteristics

Reservoir fluid inclusions were collected from the YS101, YS102, YS2, YS202, and LS2 wells. The inclusions analyzed were mostly housed in secondary microcracks which cut through quartz and feldspar grains, and partly along microfractures within quartz, created during diagenesis. The sampled hydrocarbon inclusions were mainly gas–liquid two-phase inclusions. The individual inclusions were small, mostly located in bands along secondary microcracks within quartz grains.

(1) The first member of the Quantou group: Samples were taken from the YS101, YS102, and YS202 wells, and most of the inclusions were gas–liquid two-phase inclusions with a gas–liquid ratio of <5%. The individual inclusions were small, 3–6 μm across. In these samples the majority of the inclusions were located in secondary microcracks within quartz and feldspar grains, with the rest distributed along microfractures within quartz, as created during diagenesis (Fig. 3a). (2) The Denglouku group: Samples were taken from the YS101, YS2, YS202,

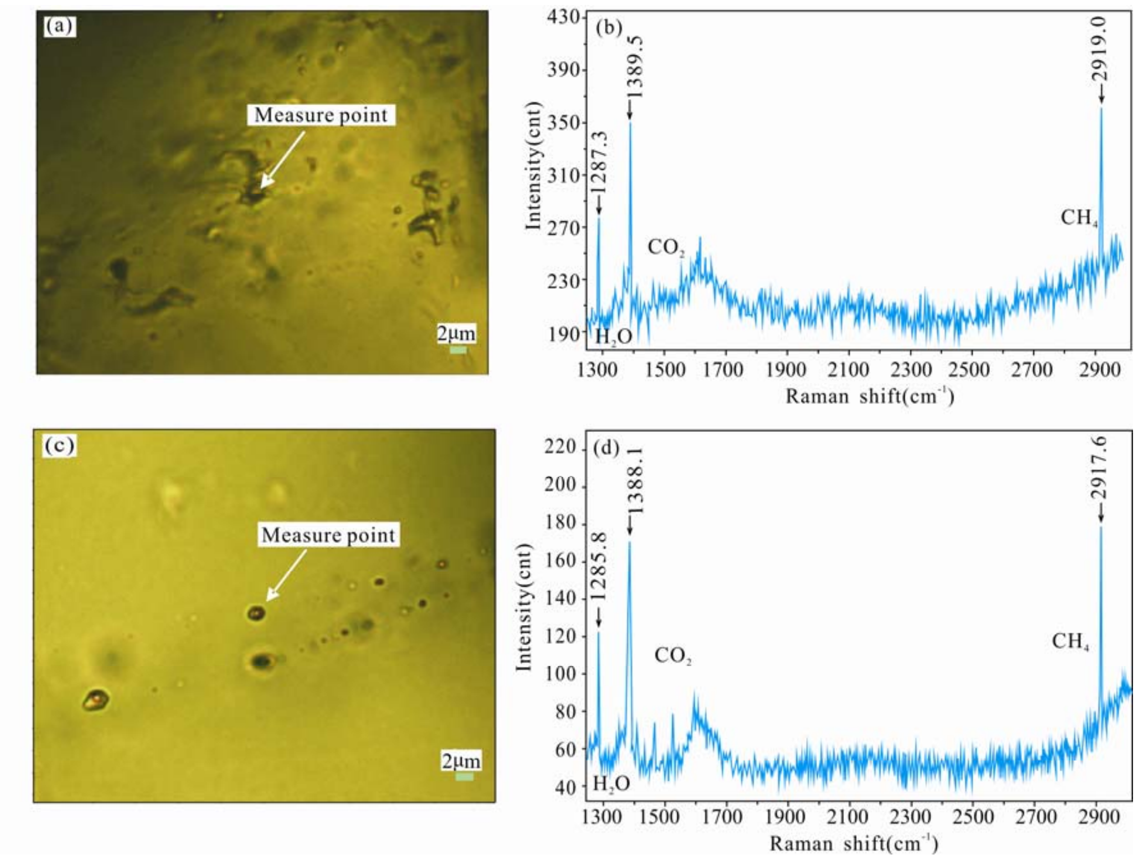

Fig. 4. Microscopic photographs of hydrocarbon-containing inclusions and the corresponding Raman spectra.
(a), Gas–liquid two–phase inclusions of YS202 well in the 3236.60 m; (b), corresponding Raman spectra in the 3236.60 m of inclusion in (a); (c), Gas-liquid two-phase inclusions of YS2 well in the 3714.74 m; (d), Corresponding Raman spectra in the 3714.74 m of inclusion in (c).

and LS2 wells. The individual inclusions were small, 3–8 μm across. In these samples the majority of the inclusions were located in secondary microcracks within quartz and feldspar, and partly hosted in sparry calcite cement (Fig. 3b). In the two–phase gas–liquid inclusions the gas–liquid ratio is <5%.

4.2 Reservoir fluid-inclusion composition

Micro laser Raman spectroscopy was used to analyze reservoir fluid inclusions to determine their composition (Chen Yong et al., 2005). The analyses were performed at the Test Research Center, Beijing Ministry of Nuclear Industry, Beijing, China, using a LABHR-VIS LabRAM HR800 micro laser Raman spectrometer with a wavelength of 532 nm, temperature of 25°C, and humidity of 50%. In general, the CH_4 and CO_2 contents of the fluid inclusions (at room temperature) gave Raman spectrum peaks at 2913–2919 cnt and 1386–1390 cnt, respectively. The samples of the first member of the Quantou group and of the Denglouku group were taken from the YS101, YS2, YS202, YS102, and LS2 wells. The microscopic fluorescent light and micro laser Raman spectroscopy analyses indicate that the types of inclusions are oil, gas, and gas–liquid two–phase inclusions.

(1) The first member of the Quantou group: Analyses of 21 inclusions showed strong blue fluorescence under fluorescent light, indicative of the presence of hydrocarbons. At a depth of 3343 m within the YS101 Well and at 3236.60 m in the YS202 well, gas–liquid two-phase inclusions were found (Fig. 4a). The main

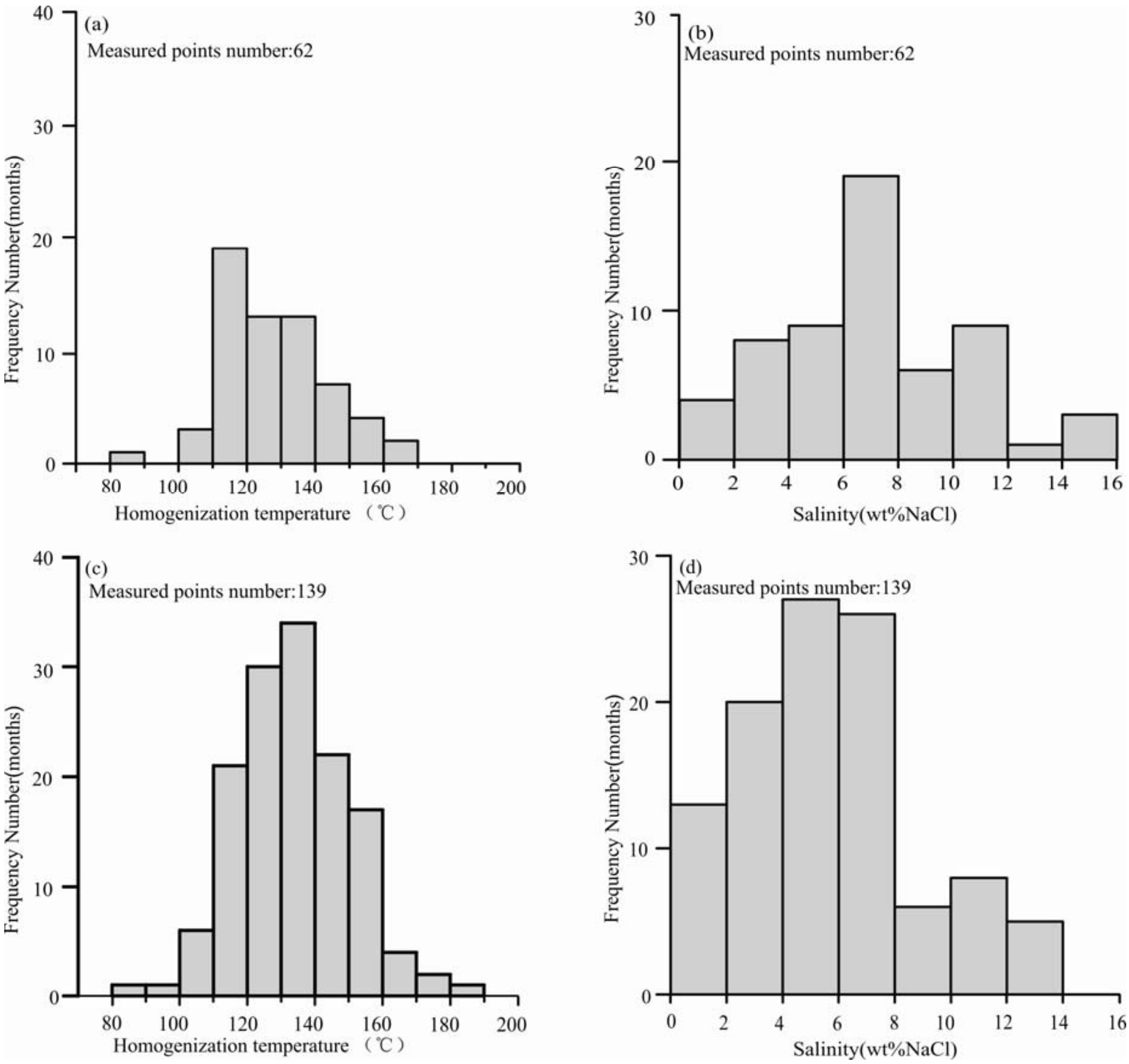

Fig. 5. Histograms of homogenization temperature and salinity for reservoir inclusions.
(a), Homogenization temperature histogram of inclusions in the first member of Quantou group; (b), Salinity inclusions histogram of inclusions in the first member of Quantou group; (c), Homogenization temperature histogram of inclusions in Denglouku group; (d), Salinity inclusions histogram of inclusions in Denglouku group.

Table 3 Reservoir fluid inclusions measured data

Horizon	Well Number	Depth (m)	Serial Number	Homogenization Temperature (℃)	Salinity (wt%NaCl)	Horizon	Well Number	Depth (m)	Serial Number	Homogenization Temperature (℃)	Salinity (wt% NaCl)	Horizon	Well Number	Depth (m)	Serial Number	Homogenization Temperature (℃)	Salinity (wt% NaCl)
The first member of Quantou group	YS101	3343.07	1	142	15.96	The first member of Quantou group	YS102	3278.35	3	123	11.05	Denglouku group	YS2	3714.74	5	153	5.26
			2	125	15.96				4	115	11.61				6	158	5.41
			3	114	15.96				5	118	11.61				7	155	5.41
			4	119	1.74				6	129	3.55				8	143	5.26
			5	115	3.23				7	121	10.33				9	146	5.26
			6	120	12.29				8	126	9.98				10	152	5.26
			7	161	6.88				9	126	9.98				11	156	5.26
			8	164	6.88				10	131	9.98				12	177	5.26
			9	136	6.88				11	123	10.04				13	160	5.26
			10	125	6.88				12	123	10.04				14	95	9.98
			11	117	3.55				13	120	9.98				15	138	2.07
			12	113	3.39				14	116	9.98				16	137	2.07
	YS202	3236.6	1	131	0.71				15	131	9.98				17	145	9.6
			2	123	0.71				16	133	10.04				18	115	9.6
			3	147	0.71				17	116	10.05				19	115	9.6
			4	151	6.01				18	120	7.36				20	118	1.57
			5	149	6.01				19	115	6.59				21	115	1.57
			6	148	6.01				20	120	6.59				22	83	1.57
			7	146	6.01				21	118	6.59		LS2	4140.6	1	132	1.74
			8	158	6.01				22	115	6.59				2	129	2.07
			9	141	5.86	Denglouku group	YS101	3538	1	115	6.74				3	123	2.07
			10	137	5.86				2	104	6.74				4	124	2.07
			11	134	5.86				3	109	6.74				5	125	2.07
			12	136	5.86				4	122	6.74				6	126	1.91
			13	140	6.16				5	110	2.9				7	127	1.91
			14	125	6.16				6	186	2.9				8	128	1.91
			15	109	4.18				7	117	1.74				9	130	1.91
			16	120	4.18				8	111	13.32				10	125	0.71
			17	133	4.18				9	119	13.32				11	124	0.71
			18	102	4.18				10	110	1.4				12	126	0.71
			19	140	4.18				11	114	12.02				13	134	4.18
			20	89	3.39				12	113	12.02				14	134	4.18
			21	127	3.39				13	111	12.02				15	135	4.18
			22	142	3.39				14	107	2.74				16	135	4.18
			23	137	3.39				15	110	2.74				17	137	4.18
			24	103	7.31				16	120	2.24				18	139	4.18
			25	124	7.31				17	116	2.24				19	137	4.18
			26	131	7.31				18	121	2.24				20	135	4.18
			27	152	7.31				1	141	5.41				21	140	4.18
			28	156	7.31				2	144	5.41				22	138	4.18
			1	120	10.77				3	148	5.41				23	136	4.03
			2	118	11.05				4	150	5.41				24	143	4.03

Table 3

Horizon	Well Number	Depth (m)	Serial Number	Homogenization Temperature (℃)	Salinity (wt% NaCl)
Denglouku group	LS2	4140.6	25	141	4.03
			26	136	4.03
			27	137	4.03
			28	139	4.03
			29	140	4.03
			30	133	4.03
			31	136	4.03
			32	138	4.03
			33	130	0.88
			34	131	0.88
	YS202	3453.86	1	113	11.19
			2	150	10.91
			3	118	10.48
			4	120	10.48
			5	125	10.62
			6	119	10.62
			7	130	10.48
			8	125	10.62
	YS202	3453.86	1	114	9.47
			2	111	9.47
			3	133	2.07
			4	140	2.07
			5	146	2.07
			6	164	2.07
			7	135	2.07
Denglouku group	YS202	3453.86	8	112	2.07
			9	170	7.31
			10	140	7.31
			11	142	7.31
			12	149	7.45
			13	146	7.45
			14	149	7.45
			15	140	7.45
			16	152	7.31
			17	160	7.31
			18	153	7.31
			19	157	7.45
			20	143	7.45
			21	149	7.45
			22	151	7.45
			23	150	7.45
			24	143	7.31
			25	152	7.31
			26	156	7.31
			27	162	7.45
			28	143	7.45
			29	160	7.31
			30	154	7.31
			31	129	0.71
			32	128	0.71
Denglouku group	YS202	3453.86	33	126	0.71
			34	123	0.71
			35	121	0.71
			36	157	3.06
			37	138	3.06
			38	132	3.06
			39	135	3.06
			40	170	3.06
			41	121	4.8
			42	125	4.96
			43	129	4.96
			44	134	4.96
			45	131	4.96
			46	127	4.8
			47	129	4.8
			48	126	4.8
			49	130	4.96
			50	152	4.96
			51	180	4.96
			52	136	4.96
			53	135	4.8
			54	127	4.8
			55	148	1.23
			56	144	1.23
			57	114	1.23

components of these two–phase inclusions were CH_4, CO_2, and H_2O (Fig. 4b). At a depth of 3236.60 m in the YS202 well, gas–liquid two–phase inclusions were found, mainly CH_4.

(2) The Denglouku group: Analyses of 28 inclusions showed strong blue fluorescence under fluorescent light, confirming the presence of hydrocarbons. At a depth of 3538 m in the YS101 well, gas–liquid two-phase inclusions were identified; the main components were CH_4 and CO_2. At a depth of 3453.86 m in the YS202 well and at 3714.74 m in the YS2 well (Fig. 4c), gas–liquid two–phase inclusions were found. CH_4 and CO_2 were dominant in the YS202 well, and CH_4, CO_2, and H_2O in the YS2 well (Fig. 4d).

4.3 Fluid inclusion temperatures

Reservoir fluid-inclusion homogenization temperatures and salinity were measured at the Beijing Ministry of Nuclear Industry using a BX51 fluorescent light microscope and a LINKAM THMS600 heater with a temperature of 24 °C and humidity of 40%. A total of 62 points were analyzed in fluid inclusions within the first member of the Quantou group, and 139 points from the Denglouku group; the results are listed in Table 3.

For the first member of the Quantou group, the reservoir fluid inclusion homogenization temperature was 89–164°C with a peak at 110–120°C; the peak frequency was 30.6% (Fig. 5a). Inclusion salinity was (0.71–15.96)wt% with a peak at (6–8)wt% (Fig. 5b). These results show that hydrocarbon accumulation in the first member of the Quantou group reservoir was a single-stage event (Gao Xianzhi et al., 2000).

For the Denglouku group, the reservoir fluid inclusion homogenization temperature was 83–186°C with a peak at 130–140°C; the peak frequency was 25.2% (Fig. 5c). Inclusion salinity was (0.71–3.32)wt% with a peak at (4–6)wt% (Fig. 5d). The results indicate that accumulation in the Denglouku group reservoir was also a single-stage event.

5 Discussion

In the field of petroleum geology, the homogenization temperature of reservoir fluid inclusions is used to study the period of hydrocarbon migration and to reconstruct the history of the reservoir. This approach is usually combined with the thermal and burial history, as once we have estimated the timing of hydrocarbon migration, we can estimate the filling time of the reservoir (Shan Xiuqin et al., 2007; Xiao Xianming et al., 2002). The burial history of the YS201 well can be drawn from the analysis above. Previous studies in the region have provided a thermal history curve. If we place the peak homogenization temperature of fluid inclusions from the first member of the Quantou group and the Denglouku group into the diagram of the burial history and thermal history, the accumulation ages of these two layers can be calculated (Yang Guang et al., 2011; Jiang Tao et al., 2010). For the first member of the Quantou group, the reservoir fluid-inclusion homogenization temperatures show a peak at 110–120°C. Placing this temperature into the burial and thermal history of the YS201 well (Fig. 6), the accumulation age of hydrocarbon reservoir is 79 Ma (middle Nenjiang group), corresponding to the middle Late Cretaceous. The hydrocarbon gas of the first member of the Quantou group reservoir migrated over a large distance. The homogenization temperature and salinity for the first member of the Quantou group both have a single peak, so this reservoir experienced a single-stage accumulation. For the Denglouku group, the reservoir fluid–inclusion homogenization temperatures also show a single peak at 130–140°C. Using this temperature value in the burial and thermal history for the YS201 well (Fig. 6), the reservoir accumulation age is 79 Ma (the middle Late Cretaceous). The similarity of the two ages indicates contemporaneous hydrocarbon migration for the reservoirs of the first member of the Quantou group and the Denglouku group. Analysis of the fluorescence of the hydrocarbon inclusions of the Denglouku group reservoir and the first member of the Quantou group reservoir indicates consistent petroleum characteristics in the hydrocarbon inclusions in the two reservoirs, indicating that both reservoirs were derived from the same source and accumulated at the same time.

6 Conclusions

(1) Using acoustic time data we calculated the denudation thickness for the Nenjiang group to be 539.18 m. Using sedimentation rates and denudation times, the denudation thicknesses for the Yingcheng and Mingshui groups are 506 m and 144.85 m, respectively.

(2) Analysis of reservoir fluid inclusions in the first member of the Quantou group yields peak values of homogenization temperature and salinity of 110–120°C and (6–8)wt%, respectively. The Denglouku group reservoir inclusions also have peak values of homogenization temperature and salinity of 130–140°C and (4–6)wt%, respectively. These values show that the accumulation of hydrocarbons occurred simultaneously in the two layers.

(3) Through combining the peak homogenization temperatures of fluid inclusions in the first member of the Quantou group and in the Denglouku group to the burial history of the YS201 well, it is determined that the two

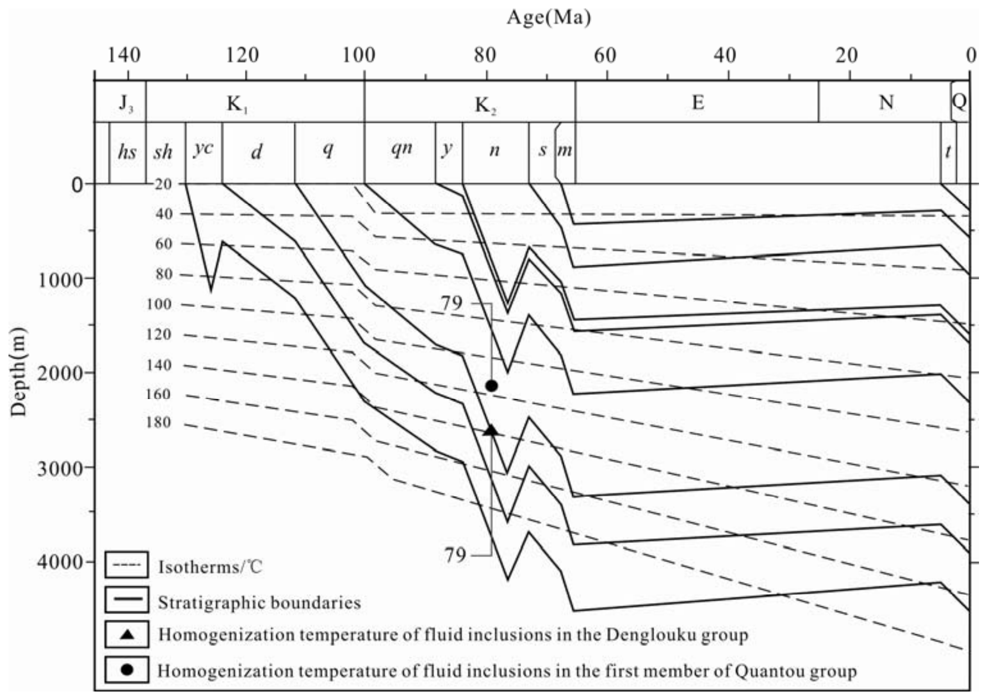

Fig. 6. Burial history of the YS201 well.

reservoirs accumulated at the same time, at 79 Ma (middle Late Cretaceous).

Acknowledgements

We thank Professor Ou Guangxi from the Beijing Nuclear Industry and Geology Institute for analyzing the fluid inclusions. This study was supported by the National Natural Science Foundation of China (grant No. 41472101).

Manuscript received Feb. 2, 2016
accepted Aug. 10, 2016
edited by Hao Qingqing

References

Bhullar, A.G., Karlsen, D.A., Backer, O.K., Seland, R.T., and Tran, K.L., 1999. Dating reservoir filling a case history from the North Sea. *Marine and Petroleum Geology*, 16: 581–603.

Bhattacharya, S., Panigrahi, M.K., and Jayananda, M., 2014. Mineral thermobarometry and fluid inclusion studies on the Close pet granite, Eastern Dharwar Craton, south India: implications to emplacement and evolution of late–stage fluid. *Journal of Asian Earth Sciences*, 91: 1–18.

Blamey, N.J.F., Azmy, K., and Brand, U., 2014. Provenance and burial history of cement in sandstones of the Northbrook Formation (Carboniferous), western Newfoundland, Canada: A geochemical investigation. *Sedimentary Geology*, 299: 30–41.

Burruss, R.C., Cerone, K.R., and Harris, P.M., 1983. Fluid inclusion petrography and tectonic burial history Al Ali No. 2 well: evidence for the timing of diagenesis and oil migration, northern Oman Fore deep. *Geology*, 11: 567–570.

Carter, A., Roques, D., and Bristow, C.S.，2000. Denudation history of onshore central Vietnam: constraints on the Cenozoic evolution of the western margin of the South China Sea. *Tectonophysics*, 322(3–4): 265–277.

Chen Juan, Zhang Qinglong, Wang Liangshu, Xie Guo'ai, Xu Shiyin, Bi Suping and Ge Rongfeng, 2008. Tectonic transformation of Changling fault depression in the southern Songliao Basin and its significance of hydrocarbon accumulation. *Acta Geologica Sinica*, 82(2): 1027–1035 (in Chinese with English abstract).

Chen Yong, Zhou Yaoqi, Liu Chaoying, Yan Yongshi and Wang Qiang, 2005. Quantitatively analyzing the homogenization process of CH_4–H_2O fluid inclusion by laser Raman spectroscopy. *Earth Science Frontiers*, 12(4):592–596 (in Chinese with English abstract).

Chen Ruiyin, Luo Xiaorong and Chen Zhankun, 2006. Estimation of denudation thickness of Mesozoic strata in the Ordos basin and its geological significance. *Acta Geologica Sinica*，80(5): 685–693 (in Chinese with English abstract) .

Chi Guoxiang, Zhou Yiming and Lu Huanzhang, 2003. An overview on current fluid-inclusion research and applications. *Acta Petrologica Sinica*, 19(2): 201–212.

Dodds, A., 2000. Migrate2: a PC program for modelling the generation, migration and accumulation of hydrocarbons in four dimensions. *Computers & Geosciences*, 26(7): 795–808.

Du Letian, Zhang Jinglian and Ou Guangxi, 2015. Reconsideration on hydrogenation and alkali-metasomatic mechanism in oil-gas genesis by mantle ichor. *Geological Review*, 61(5): 1007–1020(in Chinese with English abstract).

English, K.L., Redfern J., Corcoran D.V., English J.M., and Cherif R.Y., 2016. Constraining burial history and petroleum charge in exhumed basins: New insights from the Illizi Basin, Algeria. *AAPG Bulletin*, 100(4): 623–655.

Gao Xianzhi and Chen Fajing, 2000. Application of fluid inclusions to determination of the times and stages of hydrocarbon reservoir filling: a case study of Nanbaxian Oilfield in the Qaidamam Basin. *Earth Science Frontiers* (China University of Geosciences, Beijing), 7(4): 548–554 (in Chinese with English abstract).

Ge Rongfeng, Zhang Qinglong, Wang Liangshu, Xie Guo'ai, Xu Shiyin, Chen Juan and Wang Xiyong, 2010. Tectonic evolution of Songliao Basin and the prominent tectonic regime transition in Eastern China. *Geological Review,* 56 (2):180–195 (in Chinese with English abstract).

Goldstein, R.H., 2001. Fluid inclusions in sedimentary and diagenetic system. *Lithos*, 55: 159–193.

Grobe, A., Littke R., Sachse V., and Leythaeuser D., 2015. Burial history and thermal maturity of Mesozoic rocks of the Dolomites, Northern Italy. *Swiss Journal of Geosciences*, 108 (2–3): 253–271.

Guo Wei, Yu Wenxiang, Liu Zhaojun and Ma Lin, 2009. The burial history of the southern Songliao Basin. *Journal of Jilin University* (Earth Science Edition), 39(3): 353–360 (in Chinese with English abstract).

Haszeldine, R.S., Samson, I. M., and Cornfort, C., 1984. Dating diagenesis in petroleum basin, a new fluid inclusion method. *Nature*, 307: 354–357.

He Bizhu and Zheng Menglin, 2016. Structural characteristics and formation dynamics: a review of the main sedimentary basins in the continent of China. *Acta Geologica Sinica* (English Edition), 90(4): 1156–1194.

Henry, P.H., 1996. Analysis of sonic well logs applied to erosion estimates in the Bighorn basin, Wyomin. *AAPG Bulletin*, 80: 630–647.

Hu Ming, Fu Guang, Lü Yanfang, Fu Xiaofei and Pang Lei, 2010. The fault activity period and its relationgship to deep accumulation in the Xujiaweizi Depression, Songliao Basin. *Geological Review,* 56(5): 710–718(in Chinese with English abstract).

Ingram, G.M., Chisholm T.J., Grant C.J., Hedlund C.A., and Stuart-Smith P., 2004. Deepwater North West Borneo: hydrocarbon accumulation in an active fold and thrust belt. *Marine and Petroleum Geology*, 21(7): 897–887.

Jiang Tao and Wang Ying, 2010. Carbon dioxide accumulation stage in the Changling fault depression of the Songliao Basin. *Acta Petrologica Sinica*, 26(1): 130–134 (in Chinese).

Jones, D.M., and Machleod, G., 2000. Molecular analysis of petroleum in fluid inclusion: a practical methodology. *Org Geochem,* 31(11): 1163–1173.

Karimpouli, S., Hassani, H., Malehmir, A., Nabi-Bidhendi, M., and Khoshdel, H., 2013. Understanding the fracture role on hydrocarbon accumulation and distribution using seismic data: A case study on a carbonate reservoir from Iran. *Journal of Applied Geophy*, 96: 98–106.

Karlsen, D.A., Nedkvitne, T., Larter, S.R., and Bjorlykke, K., 1993. Hydrocarbon composition of authigenic inclusions:

application to elucidation of petroleum reservoir filling history. *Geochimica et Comochimica Acta*, 57(15): 3641–3659.

Kelly, J., Parnell, J., and Chen, H.G., 2000. Application of fluid inclusion to studies of fractured sandstone reservoirs. *Journal of Geochemical Exploration*, 69: 705–709.

Kemp, S.J., Merriman R.J., and Bouch J.E., 2005. Clay mineral reaction progress –the maturity and burial history of the Lias group of England and Wales. *Clay Minerals*, 40(1): 43–61.

Ken, L.Ferrier, and James, W. Kirchner., 2008. Effects of physical erosion on chemical denudation rates: A numerical modeling study of soil-mantled hillslopes. *Earth and Planetary Science Letters,* 272: 591–599.

Lastett, G.M., Green, P.F., Duddy, I.R., and Gleadow, A.J.W., 1987. Thermal annealing of fission tracks in apatite 2: a quantitative analysis. *Chemical Geology*, 65(1): 1–13.

Lee G.H., Kim B., Chang S.J., Huh S., and Kim H.J., 2004. Timing of trap formation in the southwestern margin of the Ulleung Basin, East Sea (Japan Sea) and implications for hydrocarbon accumulations. *Geosciences Journal*, 8(4): 369–380.

Lethaeuser, D., and Ruckheim, J., 1989. Heterogeneity of oil composition within a reservoir as a reflection of accumulation history. *Geochemica et Cosmochimica Acta*, 53: 2119–2123.

Li Zhongquan, Timoth, K., Ying Danlin, Guo Xiaoyu and Li Hongkui, 2008. Successor characteristics of the Mecozoic and Cenozoic Songliao Basins .*Acta Geologica Sinica*, 82(3): 622–628.

Liu Dehan, 1995. Fluid inclusion studies-an effective means for basin fluid investigation. *Earth Science Frontiers* (China University of Geosciences, Beijing*)*, 2(3–4):149–154 (in Chinese with English abstract).

Liu JinYan, Lin Changsong, Yu Yueyu, Wu Fadong, Jiang Liang and Chen Zhiyong, 2000. An improved method to calculation denuded amount by sonic well logs. *Petroleum Geology & Experiment*, 22(4): 302–306 (in Chinese with English abstract).

Ma Yongsheng and Zhao Peirong, 2016. Research progress in the petroleum and natural gas geological theory of China. *Acta Geologica Sinica,* 90(4):1236–1248.

Mark, D.F., Parnell, J., Kelley, S.P., Lee, M., Sherlock, S.C., and Carr, A., 2005. Dating of multistage fluid flow in sandstones. *Science*, 309: 2048–2051.

Mark, D.F., Parnell, J., Kelley, S.P., and Sherlock, S.C., 2006. Temperature–composition–time (*T–X–t*) data from authigenic K–feldspar: An integrated methodology for dating fluid flow events. *Journal of Geochemical Exploration*, 89: 259–262.

Mu Zhonghai, Chen Zhiyong, Lu Tingqing, You Fubao and Li Deqi, 2000. Erosion thickness recovery of Northern Qaidam Basin in Mesozoic. *Petroleum Exploration and Development*, 27(1):35–37 (in Chinese with English abstract).

Munz, I.A., Wangen, M., Girard, J.P., Lacharpagne, J.C., and Johansen, H., 2004. Pressure temperature time composition (P Tt X) constraints of multiple petroleum charges in the Hild field, Norwegian North Sea. *Marine and Petroleum Geology*, 21: 1043–1060.

Nedkvitne, T., Karlsen, D.A., Bjorlykke, K., and Larter, S.R., 1993. Relationship between reservoir diagenetic evolution and petroleum emplacement in the Ula Field, North Sea. *Mar.Petrol.Geol*, 10: 255–270.

Pang Xiongqi, Jia Chengzao and Wang Wenyang, 2015. Petroleum geology features and research developments of hydrocarbon accumulation in deep petroliferous basins. *Petroleum Science,* 12:1–53.

Premarathne, U., Suzuki, N., Ratnayake, N., and Kularathne, C., 2016. Burial and thermal history modelling of the Mannar Basin, Offshore Sri Lanka. *Journal of Petroleum Geology*, 39 (2): 193–213.

Punanova, S.A., and Vinogradova T.L., 2006. Prediction of the phase state of hydrocarbon accumulations in the mesozoic deposits of northwestern Siberia. *Geochemistry International*, 44(9): 912–924.

Raznitsin, Y.N., 2014. The petroleum potential and a geodynamic model for the formation of hydrocarbon accumulations on the southern shelf of Cuba. *Doklady Earth Sciences*, 456(2): 685–688.

Shan Xiuqin, Chen Honghan and Luo Xia, 2007. Studying hydrocarbon accumulation history of Ordos Upper-Paleozoic by fluid inclusion analysis. *Acta Petrologica Sinica*, 23(9): 2303–2309 (in Chinese with English abstract).

Sachse, V.F., Anka, Z., Littke, R., Horsfield, B., and Primio, R., 2016. Burial, temperature and maturation history of the Austral and Western Malvinas Basins, Southern Argentina, based on 3D basin modelling. *Journal of Petroleum Geology*, 39(2): 169–191.

Tan Kaijun and Mu Zhonghai, 2004. Restoration of erosion thickness of Upper Cambrian–Ordovician in Southwest area of Tarim Basin. *Henan Petroleum*, 18(3): 4–6 (in Chinese with English abstract).

Tokatli, K., Demirel I.H., and Karayigit A.I., 2006. Burial history and thermal maturity assessment of Upper Cretaceous –Lower Tertiary formations in the Cankiri Basin, Turkey. *International Journal of Coal Geology*, 66: 1–2.

Wang Pujun, Xie Xiao'an, Mattern, F., Ren Yanguang, Zhu Defang and Sun Xiaomeng, 2007. The Cretaceous Songliao basin: volcanogenic succession, sedimentary sequence and tectonic evolution, NE China. *Acta Geologica Sinica* (English Edition)*,* 81(6):1002–1011.

Wang Yougong, Lü Yanfang, Fu Guang, Sun Yonghe and Li Xin, 2014. Growth characteristic of boundary control faults and its significance to oil and gas geology. *Acta Geologica Sinica,* 88(9): 1666－1675(in Chinese with English abstract).

Xiang Caifu, Feng Zhiqiang, Pang Xiongqi, Wu Heyong and Li Junhong, 2007. Advanced thermal history and tectonic significance of the Songliao Basin: evidence from apatite fission track (AFT). *Science in China* (Series D), 38(8): 1024–1031 (in Chinese).

Xiao Xianming, Liu Zufa, Liu Dehan, Mi Jingkui, Shen Jiagui and Song Zhiguang, 2002. Application of reservoir fluid inclusions Information Studies natural gas accumulation in time. *Chinese Science Bulletin*, 47(12):957–960 (in Chinese).

Yan Baozhen, Zhu Yanming, Zhao Hong, Tang Xingwen and Tang Kun, 2006. Computer model for reconstruction of basin burial history: a preliminary discussion on application of object-oriented methodology. *Gas Industry*, 26(1):37–39 (in Chinese with English abstract).

Yang Guang, Zhao Zhanyin and Shao Mingli, 2011. Formation of carbon dioxide and hydrocarbon gas reservoirs in the Changling fault depression, Songliao Basin. *Petroleum Exploration and Development*, 38(1): 42–48.

Yuan Yusong, Zheng Herong and Tu Wei, 2008. Methods of eroded strata thickness restoration in sedimentary basins.

Petroleum Geology and Experiment, 30(6): 636–642 (in Chinese with English abstract).

Zhao Mengjun, Song Yan, Pan Wenqing, Han Jianfa, Liu Shaobo and Qin Shengfei., 2004. The overall approach of hydrocarbon filling periods and process in sedimentary basins. *Advances in Earth Science*, 19(6): 939–946 (in Chinese with English abstract).

Zhao Wenzhi and Li Jianzhong, 2004. Control of basement faults on hydrocarbon accumulation in Southern Songliao Basin. *Acta Petrolei Sinica*, 25(4): 1–6 (in Chinese with English abstract).

Zheng Youye, Li Xiaojü, Ma Lijuan and Lin Songhui, 1998. Application status of organic inclusion in the research on oil generation basin. *Earth Science Frontiers*, 5(1–2): 325–331 (in Chinese with English abstract).

Zou Caineng, Tao Shizhen and Zhang Youyu, 2007. Reservoir–forming age and its exploration significance to stratigraphic reservoirs in southern Songliao Basin. *Chinese Science Bulletin*, 52(23): 3239–3252.

About the first author

YANG Guang, female; born in 1957; Professor of Jilin University, engaged in teaching and research work of oil and gas resource exploration.E-mail: yg@jlu.edu.cn.